  Bull. Chem. Soc. Jpn., 56, 1753—1760 (1983)

Structure of the Electrical Double Layer at the Interface between Nitrobenzene Solution of Tetrabutylammonium Tetraphenylborate and Aqueous Solution of Lithium Chloride

Takashi KAKIUCHI and Mitsugi SENDA*

Department of Agricultural Chemistry, Faculty of Agriculture, Kyoto University, Sakyo-ku, Kyoto 606

(Received December 22, 1982)

Electrocapillary curves at the polarized interface between a nitrobenzene solution of tetrabutylammonium tetraphenylborate (TBATPB) and an aqueous solution of lithium chloride at various concentrations of TBATPB and LiCl have been measured by the drop time method using a dropping electrolyte solution electrode at 25 °C. The relative surface excesses of tetrabutylammonium and tetraphenylborate ions in the nitrobenzene phase and of lithium and chloride ions in the aqueous phase were well described by the Gouy-Chapman theory of diffuse layers for both sides of the interface. A model of the electrical double layer for the nitrobenzene–water interface is presented, in which an ion-free inner layer consisting of laminated monolayers of water and nitrobenzene is sandwiched by the two diffuse layers on each side of the interface. The potential difference across the inner layer, which was estimated to be *ca.* 20 mV at the potential of zero charge, was found to be dependent on the surface charge density and to be nearly independent of the electrolyte concentration.

In a previous paper[1] we have reported the experimental conditions under which the interface between a nitrobenzene solution of tetrabutylammonium tetraphenylborate (TBATPB) and an aqueous solution of lithium chloride behaves as a polarized interface. Such an interface is amenable to a study of its double structure based on the thermodynamics of an ideal polarized interface between two immiscible electrolyte solutions. Watanabe *et al.*[2] first applied the concept of ideal polarizability to the oil–water interfaces in order to analyze their double layer structure. At such interfaces, however, there always existed a significant amount of ion transfer current through the interface, so that the precise control of the electrical potential difference across the interface was not achieved. Gavach *et al.*[3,4] have studied the double layer structure of the non-polarized nitrobenzene–water interfaces by surface tension measurements. They have shown that the Gouy-Chapman theory of diffuse double layers well describes their experimental results when no specific adsorption of ions at the interface was assumed. In a non-polarized interface, however, the specific adsorption of ions cannot be detected from the electrocapillary measurements, since the surface charge density and surface excesses of ions cannot be independently determined.

In this paper, we describe the results of the experimental study of the double layer structure at the polarized interface between a nitrobenzene solution of TBATPB and an aqueous solution of LiCl on the basis of the electrocapillary measurements and we present an electrical double layer model of the interface. Electrocapillary curves of a polarized interface, in conjunction with the thermodynamics of ideal polarized interface between two immiscible electrolyte solutions[5] and with the Gouy-Chapman theory of electrical double layer, provide us an unequivocal way to examine the adsorption of ions at the interface by determining the surface charge density and surface excesses of individual ionic species.

Experimental

The interfacial tension at the polarized interface between the nitrobenzene solution of TBATPB and the aqueous solution of LiCl was measured with the drop time method using a dropping electrolyte solution electrode.[1] The aqueous lithium chloride solution was dropped upward into the nitrobenzene solution from the tip of a poly(tetrafluoroethylene) capillary of 0.5 mm inner diameter. The flow rate of the aqueous solution and the drop time were typically 0.00036 ml s^{-1} and 50 s. The potential drop across the interface was controlled using a four-electrode potentiostat with a positive feedback device for IR compensation.[6] Details of the measurements and the calculation of the surface tension from the drop time have been reported elsewhere.[1] All the measurements were made at 25.00±0.05 °C in the dark.

TBATPB, tetrabutylammonium chloride (TBACl) and nitrobenzene were purified as described elsewhere.[1] Lithium chloride(spurapur grade, E. Merck) was dissolved into twice distilled water to prepare the stock solution. The concentration of LiCl was determined potentiometrically using a standard silver nitrate solution. Aqueous LiCl solutions of desired concentrations were prepared by serial dilution of the stock solution. Nitrobenzene solutions of TBATPB were prepared in the dark immediately before use.

Results

The electrochemical cell employed in this study is represented by

I	II	III	IV	V
Ag	AgCl	a mol dm^{-3} TBACl	b mol dm^{-3} TBATPB	c mol dm^{-3} LiCl
		(water)	(nitrobenzene)	(water)

VI	VII
AgCl	Ag.

(I)

The interface between phases IV and V is the polarized nitrobenzene–water interface which we are concerned with. The nitrobenzene–water interface between phases III and IV is a non-polarized interface where the potential drop across the interface is determined by the activities of TBA^+ ions in the phases III and IV.[7-9] The electrocapillary equation for the present system at constant temperature and pressure takes the form[5]

$$-d\gamma = q^{W}dE_{0^+}^{W^-} + \Gamma_{Li/W}d\mu_{LiCl} + \Gamma_{TPB/NB}d\mu_{TBATPB}, \quad (1)$$

where $\Gamma_{Li/W}$ and $\Gamma_{TPB/NB}$ are the relative surface concentrations (the relative surface excesses) of Li^+ and TPB^- ions defined by

$$\Gamma_{Li/W} = \Gamma_{Li} - \frac{x_{NB}^{NB}\Gamma_W - x_W^{NB}\Gamma_{NB}}{x_W^W x_{NB}^{NB} - x_W^{NB} x_{NB}^W} x_{LiCl}^W, \quad (2)$$

and

$$\Gamma_{TPB/NB} = \Gamma_{TPB} - \frac{x_W^W\Gamma_{NB} - x_{NB}^W\Gamma_W}{x_W^W x_{NB}^{NB} - x_W^{NB} x_{NB}^W} x_{TBATPB}^{NB}. \quad (3)$$

Here, γ is the interfacial tension, q^W the surface charge density in aqueous phase defined by $q^W = F(\Gamma_{Li} - \Gamma_{Cl})$, F being the Faraday. x_i^α, μ_i^α, and Γ_i denote the mole fraction, the chemical potential and the surface concentration (the amount of matter in unit area of the interphase),[10] respectively, of i component in α phase (α= NB : nitrobenzene or W : aqueous phase). E_{O+}^{W-} is the potential of the right hand side terminal of the cell (I) with respect to the left, and the subscript O+ and superscript W− on E indicate that the reference electrodes in the nitrobenzene and aqueos phases are reversible to a cation (TBA^+) and an anion (Cl^-), respectively. Since x_W^{NB} and x_{NB}^W are 0.0175 and 0.000295, respectively, for water and nitrobenzene in the absence of an electrolyte at 25 °C,[11] Eqs. 2 and 3 can be approximated by[12]

$$\Gamma_{Li/W} = \Gamma_{Li} - \frac{x_{LiCl}^W}{x_W^W}\Gamma_W, \quad (4)$$

and

$$\Gamma_{TPB/NB} = \Gamma_{TPB} - \frac{x_{TBATPB}^{NB}}{x_{NB}^{NB}}\Gamma_{NB}. \quad (5)$$

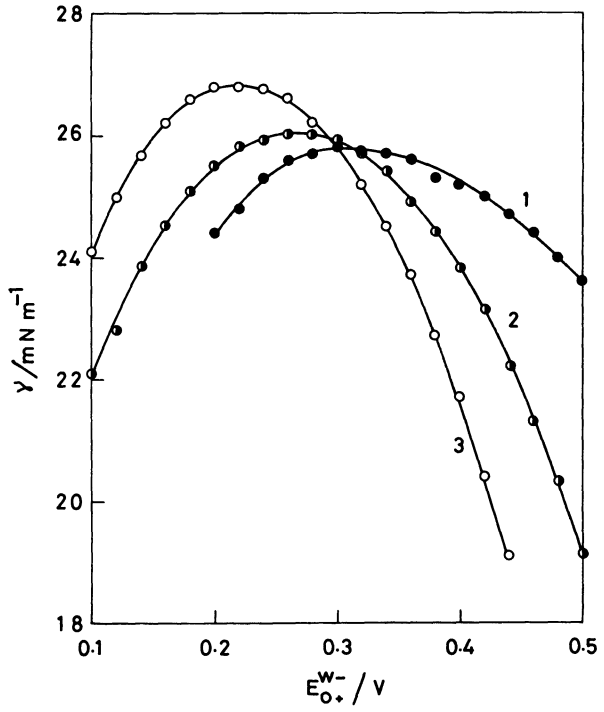

Fig. 1. Electrocapillary curves for the interface between nitrobenzene solution of 0.1 mol dm^{-3} tetrabutylammonium tetraphenylborate and aqueous solution of (1): 0.01, (2): 0.10, and (3): 1.00 mol dm^{-3} lithium chloride at 25 °C.

TABLE 1. COORDINATES OF ELECTROCAPILLARY MAXIMUM FOR THE INTERFACE BETWEEN NITROBENZENE SOLUTION OF 0.1 mol dm^{-3} TETRABUTYLAMMONIUM TETRAPHENYLBORATE AND AQUEOUS SOLUTION OF 0.01 TO 1.0 mol dm^{-3} LITHIUM CHLORIDE AT 25 °C

c_{LiCl}^W / mol dm^{-3}	$a_{\pm,LiCl}^W$	γ_{pzc} / mN m^{-1}	E_{pzc} / V
0.01	0.009	25.8	0.309
0.02	0.017	25.7	0.289
0.05	0.041	25.8	0.278
0.10	0.079	26.0	0.265
0.20	0.151	26.2	0.245
0.50	0.369	26.5	0.227
1.00	0.776	26.8	0.217

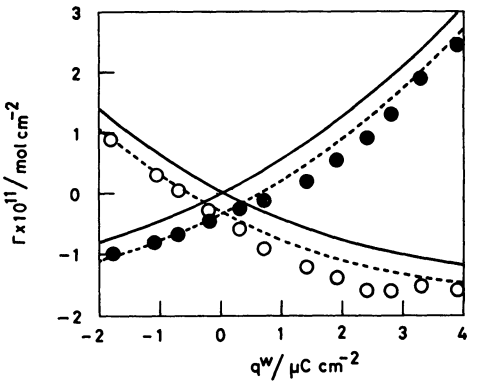

Fig. 2. Relative surface excesses of lithium ion (●) and chloride ion (○) in the aqueous phase as a function of the surface charge density in aqueous phase at 0.1 mol dm^{-3} lithium chloride. The solid lines are the theoretical curves based on Gouy-Chapman theory. Dashed lines are the curves corrected for the exclusion of lithium and chloride ions from the inner layer.

Aqueous Phase. Electrocapillary curves were measured for seven different concentrations of LiCl, c=0.01 to 1.00 mol dm^{-3}, at a=0.1 mol dm^{-3} and b= 0.1 mol dm^{-3} in the cell (I). Some of the results are shown in Fig. 1. The coordinates of the electrocapillary maximum are given in Table 1. The potential of zero charge, E_{pzc}, and the interfacial tension at the potential of zero charge, γ_{pzc}, were determined by a least square fit of an electrocapillary curve around the maximum to a third order polynomial. The mean molar ionic activity of LiCl, $a_{\pm,LiCl}^W$, in Table 1 was calculated from Davies' extended equation[13] of the Debye-Hückel theory for the concentrations below 0.1 mol dm^{-3} and was taken from the literature data[14] for the concentrations above 0.1 mol dm^{-3}.

Using Eq. 1, we obtained q^W by numerical differentiation of the electrocapillary curves with respect to E_{O+}^{W-}. $\Gamma_{Li/W}$ was calculated from numerical differentiation of γ *vs.* log $a_{\pm,LiCl}^W$ curves with respect to log $a_{\pm,LiCl}^W$. The relative surface excess of Cl^- ion, $\Gamma_{Cl/W}$, was evaluated by $q^W = F(\Gamma_{Li} - \Gamma_{Cl}) = F(\Gamma_{Li/W} - \Gamma_{Cl/W})$. Figure 2 shows $\Gamma_{Li/W}$ and $\Gamma_{Cl/W}$ for 0.1 mol dm^{-3} LiCl as a function of q^W.

Nitrobenzene Phase. Electrocapillary curves were measured for seven different concentrations of TBATPB

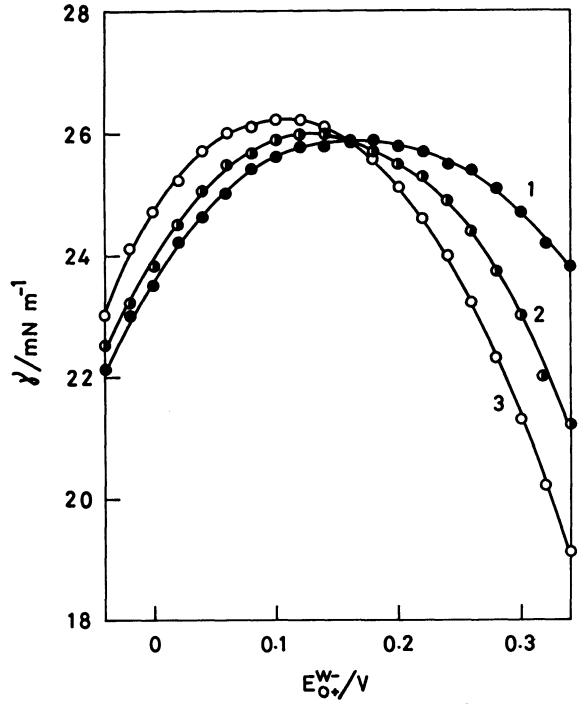

Fig. 3. Electrocapillary curves for the interface between aqueous solution of 0.1 mol dm^{-3} lithium chloride and nitrobenzene solution of (1): 0.02, (2): 0.05, and (3): 0.17 mol dm^{-3} tetrabutylammonium tetraphenylborate at 25 °C.

Table 2. Coordinates of electrocapillary maximum for the interface between aqueous solution of 0.1 mol dm^{-3} lithium chloride and nitrobenzene solution of 0.01 to 0.17 mol dm^{-3} tetrabutylammonium tetraphenylborate at 25 °C

c^{NB}_{TBATPB} / mol dm^{-3}	$a^{\pm,NB}_{TBATPB}$	γ_{pzc} / mN m^{-1}	E_{pzc} / V
0.01	0.008	25.9	0.167
0.02	0.014	25.9	0.153
0.03	0.021	26.0	0.142
0.05	0.033	26.0	0.131
0.07	0.044	26.0	0.129
0.10	0.061	26.1	0.122
0.17	0.099	26.3	0.108

in the nitrobenzene phase, b=0.01 to 0.17 mol dm^{-3}, at a=0.005 mol dm^{-3} and c=0.1 mol dm^{-3} in the cell (I). Some of the results are shown in Fig. 3. The concentration of TBACl in phase III in the cell (I) was kept at such a low value to ensure that the potential across the interface between the phases III and IV would show a Nernstian response for the activity of TBA$^+$ ion in the nitrobenzene phase[9] in the concentration range of TBATPB. Separate measurements showed that the potential of this reference electrode was 0.145 V more negative than that of the reference electrode with 0.1 mol dm^{-3} TBACl used in the measurements of ion adsorption in the aqueous phase.

The coordinates of the electrocapillary maximum are given in Table II. To check the degree of the association

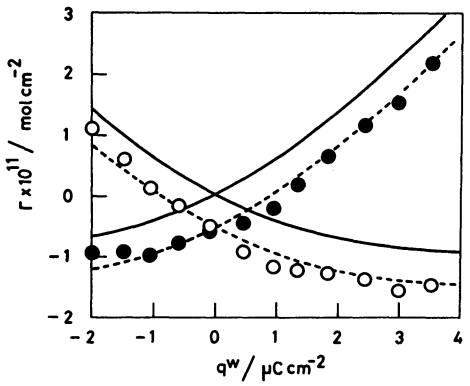

Fig. 4. Relative surface excesses of tetrabutylammonium (○) and tetraphenylborate (●) ions in the nitrobenzene phase as a function of the surface charge density in the aqueous phase at 0.1 mol dm^{-3} tetrabutylammonium tetraphenylborate.

of TBA$^+$ and TPB$^-$ ions in water-saturated nitrobenzene, the conductance of a series of the TBATPB solutions was measured. No indication of the association of the ions was observed in the concentration range used in the electrocapillary measurements. The mean molar ionic activity of TBATPB in the nitrobenzene phase was calculated using the Debye-Hückel theory allowing for a finite size of the ions;[14] here an apparent diameter, 10 Å, was assumed for TBA$^+$ and TPB$^-$ ions.[15] The surface charge density and relative surface excesses of TBA$^+$ and TPB$^-$ ions ($\Gamma_{TBA/NB}$ and $\Gamma_{TPB/NB}$) were calculated similarly. $\Gamma_{TBA/NB}$ and $\Gamma_{TPB/NB}$ at 0.1 mol dm^{-3} TBATPB are plotted against q_W in Fig. 4.

Discussion

We consider that the nitrobenzene–water interface consists of an inner layer which is sandwiched by the two diffuse double layers in the nitrobenzene and the aqueous solution sides.

Ion Adsorption in Aqueous Solution Side. The relative surface excess of Li$^+$ ions defined by Eq. 4 may be divided formally into two parts, that is, the relative surface excess in the inner layer, ${}^{i}\Gamma_{Li/W}$, and that in the diffuse layer, ${}^{d}\Gamma_{Li/W}$;

$$\Gamma_{Li/W} = {}^{i}\Gamma_{Li/W} + {}^{d}\Gamma_{Li/W}, \quad (6)$$

with

$${}^{i}\Gamma_{Li/W} = {}^{i}\Gamma_{Li} - \frac{x^{W}_{LiCl}}{x^{W}_{W}} {}^{i}\Gamma_{W}, \quad (7)$$

and

$${}^{d}\Gamma_{Li/W} = {}^{d}\Gamma_{Li} - \frac{x^{W}_{LiCl}}{x^{W}_{W}} {}^{d}\Gamma_{W}, \quad (8)$$

where ${}^{i}\Gamma_j$ and ${}^{d}\Gamma_j$ (j=Li for lithium ion and W for water) are the surface amounts of j in the inner layer and diffuse layer, respectively, per unit surface area. If we assume that the number of moles of water molecules per unit volume in the diffuse layer, ${}^{d}n^{W}_{W}$, is constant and equal to that in the bulk of the solution, ${}^{b}n^{W}_{W}$, we may write

$${}^{d}\Gamma_{Li/W} = \int_{x=x_2}^{x=\delta} ({}^{d}n^{W}_{Li} - {}^{b}n^{W}_{Li}) dx, \quad (9)$$

where ${}^{d}n_{Li}^{W}$ and ${}^{b}n_{Li}^{W}$ are the number of moles of Li^+ ion per unit volume in the diffuse layer and that in the bulk of the solution, respectively, and the integration extends from the outer Helmholtz plane ($x=x_2$) to the boundary plane of the interphase ($x=\delta$) where the composition is identical with that of the bulk of the solution. Similarly, for a Cl^- ion we may write

$$\Gamma_{Cl/W} = {}^{i}\Gamma_{Cl/W} + {}^{d}\Gamma_{Cl/W}, \tag{10}$$

with

$${}^{i}\Gamma_{Cl/W} = {}^{i}\Gamma_{Cl} - \frac{x_{LiCl}^{W}}{x_{W}^{W}} {}^{i}\Gamma_{W}, \tag{11}$$

and

$${}^{d}\Gamma_{Cl/W} = {}^{d}\Gamma_{Cl} - \frac{x_{LiCl}^{W}}{x_{W}^{W}} {}^{d}\Gamma_{W}, \tag{12}$$

and also

$${}^{d}\Gamma_{Cl/W} = \int_{x=x_2}^{x=\delta} ({}^{d}n_{Cl}^{W} - {}^{b}n_{Cl}^{W})dx. \tag{13}$$

The relative surface excesses of Li^+ and Cl^- ions in the diffuse layer defined by Eqs. 8 and 12 can be calculated from the Gouy-Chapman theory and are given, respectively, by ${}^{d}\Gamma_{+}^{W}$ and ${}^{d}\Gamma_{-}^{W}$ as follows:

$${}^{d}\Gamma_{\pm}^{W} = \frac{A^W}{F}\left(\pm\frac{q^W - {}^{i}q^W}{2A^W} + \sqrt{\left(\frac{q^W - {}^{i}q^W}{2A^W}\right)^2 + 1} - 1\right). \tag{14}$$

Here, ${}^{i}q^{W}$ is the charge density in the inner layer of the aqueous solution side and $A^W=(2RT\varepsilon^W c_{LiCl}^{W})^{1/2}$, where ε^W is the permittivity of water and c_{LiCl}^{W} is the concentration of LiCl. When all the ions are excluded from the inner layer, *i.e.*, in the case of an ion-free inner layer or of no specific adsorption of ions, ${}^{i}\Gamma_{Li}$, ${}^{i}\Gamma_{Cl}$, and ${}^{i}q^{W}$ reduce to zero. The calculated ${}^{d}\Gamma_{\pm}^{W}$ *vs.* q^W curves when ${}^{i}q^{W}=0$, $c_{LiCl}^{W}=0.1$ mol dm^{-3} and $\varepsilon^W=6.5\times10^{-10}$ F m^{-1} are shown by solid lines in Fig. 2. We estimated ${}^{i}\Gamma_{W}$ to be 1.73×10^{-9} mol cm^{-2}, assuming that the density of water in the inner layer is equal to that in the bulk of water and that the inner layer has the thickness of a monomolecular layer of water. Thus, ${}^{i}\Gamma_{Li/W}={}^{i}\Gamma_{Cl/W}=-(x_{LiCl}^{W}/x_{W}^{W}){}^{i}\Gamma_{W}=-3.1\times10^{-12}$ mol cm^{-2} when $c_{LiCl}^{W}=0.1$ mol dm^{-3}. The dashed lines in Fig. 2 are the calculated curves of the relative surface excess of Li^+ and Cl^- ions obtained by shifting the solid lines by this amount of $-(x_{LiCl}^{W}/x_{W}^{W}){}^{i}\Gamma_{W}$. The experimental relative surface excesses agree fairly well with the calculated curves for both Li^+ and Cl^- ions. Thus, the results in Fig. 2 can reasonably be explained by assuming the existence of an ion free inner layer, *i.e.*, the absence of specific adsorption of ions, in the aqueous solution side of the interface.

The variation of γ_{pzc} with $\ln(a_{LiCl}^{\pm,W})$ can be calculated from the integral form of Eq. 1:

$$\gamma_{pzc} = (\gamma_{pzc})_{c_{LiCl}^{W}=0.1} + 2RT\int_{\ln(0.079)}^{\ln(a_{LiCl}^{\pm,W})} -(x_{LiCl}^{W}/x_{W}^{W}){}^{i}\Gamma_{W}\,d\ln(a_{LiCl}^{\pm,W}), \tag{15}$$

when ${}^{i}\Gamma_{Li}={}^{i}\Gamma_{Cl}=0$ at the pzc. In Eq. 15 R and T have the usual meanings. The lower limit of the integration corresponds to $\ln(a_{LiCl}^{\pm,W})$ at $c_{LiCl}^{W}=0.1$ mol dm^{-3}. The observed increase of γ_{pzc} with the increase in $\ln(a_{LiCl}^{\pm,W})$ is well reproduced by Eq. 15, as shown in Fig. 5.

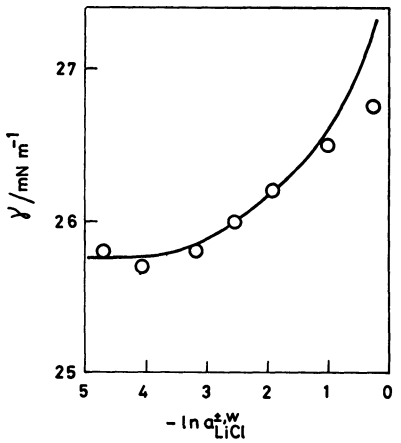

Fig. 5. Variation of interfacial tension at the potential of zero charge with the change of the activity of lithium chloride. Solid line is the calculated curve assuming the exclusion of lithium and chloride ions from the inner layer.

Figure 6 shows E_{0+}^{W-} values plotted against $\ln(a_{LiCl}^{\pm,W})$ at several different q^W values. The slope of these plots, analogous to the Esin-Markov coefficient at the mercury-solution interface,[16] is given by

$$\left(\frac{\partial E_{0+}^{W-}}{\partial \ln(a_{LiCl}^{\pm,W})}\right)_{q^W,\mu_{j\neq LiCl}} = -2RT \times\left[\left(\frac{\partial {}^{d}\Gamma_{Li/W}}{\partial q^W}\right)_{\mu_j} + \left(\frac{\partial {}^{i}\Gamma_{Li}}{\partial q^W}\right)_{\mu_j} - \frac{x_{LiCl}^{W}}{x_{W}^{W}}\left(\frac{\partial {}^{i}\Gamma_{W}}{\partial q^W}\right)_{\mu_j}\right]. \tag{16}$$

When both the presence of the ions in the inner layer and the dependence of ${}^{i}\Gamma_{W}$ on q^W are negligible, the coefficient is given by the first term of the right hand side of Eq. 16, which can be calculated from the Gouy-Chapman theory; from Eq. 14 we have

$$\left(\frac{\partial {}^{d}\Gamma_{Li/W}}{\partial q^W}\right)_{\mu_j} = \frac{1}{F}\left(1+\frac{q^W/2}{[(q^W/2)^2+(A^W)^2]^{1/2}}\right). \tag{17}$$

Therefore, in the case of the absence of specific absorption of ions, the coefficient is expected to become $-2RT/F$, $-RT/F$ and 0 when $q^W\gg0$, $q^W=0$, and $q^W\ll0$, respectively. The experimental plot at the pzc in Fig. 6 is a straight line with the slope of -23 mV which is close to $-RT/F=-25.6$ mV at 25 °C. The small difference might be attributable to a slight dependence of ${}^{i}\Gamma_{W}$ on q^W and/or a weak specific adsorption of ions in the inner layer. Figure 6 shows that the slope becomes larger with the positive increase of q^W, which is consistent with the prediction of Eq. 15.

We calculated the potential at the outer Helmholtz plane in the aqueous solution side (OHP(W)), ϕ_2^W, referred to the inner potential of the bulk of the aqueous solution, ϕ^W, by using the Gouy-Chapman theory:

$$\phi^W - \phi_2^W = \frac{2RT}{F}\sinh^{-1}[q^W/(2A^W)]. \tag{18}$$

In Fig. 7 $\phi^W-\phi_2^W$ is plotted against the rational potential,[17] $E_{0+}^{W-}-E_{pzc}$, at three different concentrations of LiCl. The variation of $\phi^W-\phi_2^W$ with $E_{0+}^{W-}-E_{pzc}$ is much smaller than those usually observed at the mercury-

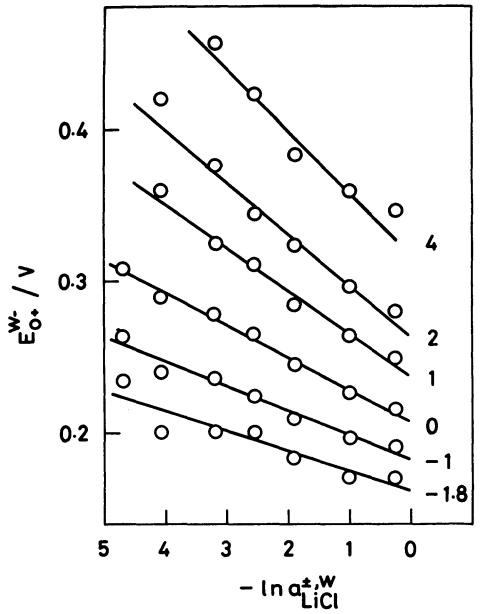

Fig. 6. Esin-Markov plots for aqueous solution phase in contact with nitrobenzene solution of 0.1 mol dm^{-3} tetrabutylammonium tetraphenylborate. The surface charge density in aqueous phase is indicated by each line in μC cm^{-2}.

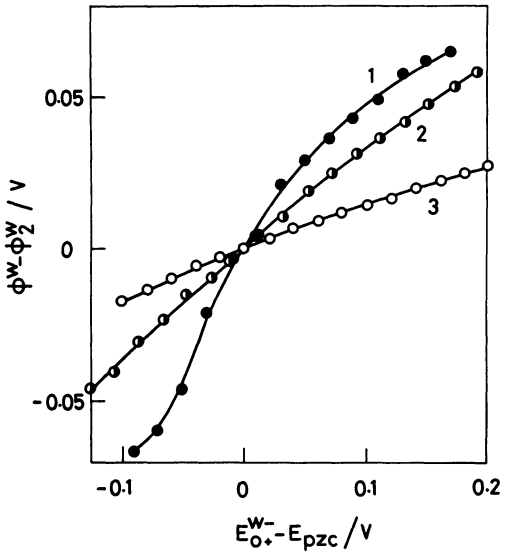

Fig. 7. Potential at the outer Helmholtz plane in aqueous solution side of the interface as a function of rational potential difference at (1): 0.01, (2): 0.1, and (3): 1.0 mol dm^{-3} lithium chloride.

aqueous solution interface in the absence of specific adsorption of ions.[18]

Ion Adsorption in Nitrobenzene Solution Side. The relative surface excesses of TBA^+ and TPB^- ions in the diffuse layer in the nitrobenzene solution side were calculated under the assumption of the ion-free inner layer from the Gouy-Chapman theory:

$$ {}^{d}\Gamma^{o}_{\pm} = \frac{A^{NB}}{F}\left[\mp\frac{q^W - {}^{i}q^W}{2A^{NB}}\sqrt{\left(\frac{q^W - {}^{i}q^W}{2A^{NB}}\right)^2+1} - 1\right]. \quad (19) $$

In Eq. 19 ${}^{d}\Gamma^{o}_{+}$ and ${}^{d}\Gamma^{o}_{-}$ are the surface excesses of TBA^+ and TPB^- ions, respectively, in the diffuse layer,

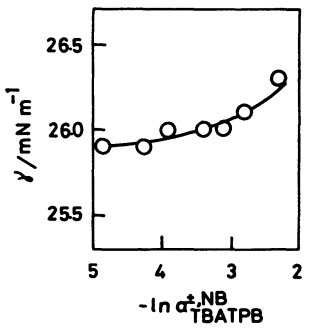

Fig. 8. Variation of interfacial tension at the potential of zero charge with the change of the activity of tetrabutylammonium tetraphenylborate. Solid line is the calculated curve assuming the exclusion of tetrabutylammonium and tetraphenylborate ions from the inner layer.

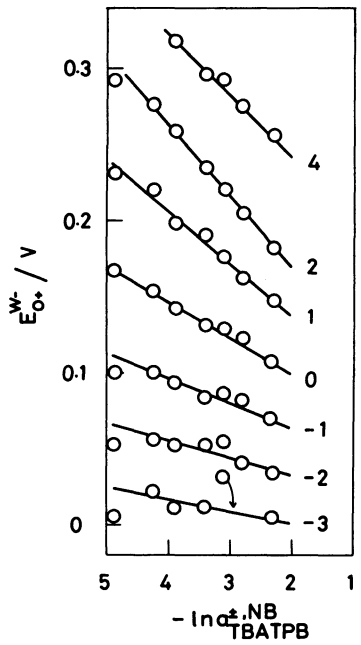

Fig. 9. Esin-Markov plots for nitrobenzene solution phase in contact with aqueous solution of 0.1 mol dm^{-3} lithium chloride. The surface charge density in aqueous phase is indicated by each line in μC cm^{-2}.

and $A^{NB}=(2RT\varepsilon^{NB}c^{NB}_{TBATPB})^{1/2}$ where ε^{NB} and c^{NB}_{TBATPB} are the permittivity of nitrobenzene and the concentration of TBATPB in the nitrobenzene phase. The solid lines in Fig. 4 are the curves calculated according to Eq. 19, when ε^{NB} and c^{NB}_{TBATPB} are 3.08×10^{-9} F m^{-1} and 0.1 mol dm^{-3}, respectively. The number of moles of nitrobenzene molecules in the inner layer per unit surface area was estimated to be 5.40×10^{-10} mol cm^{-2}. The dashed lines in Fig. 4 are the calculated curves corrected for the exclusion of ions from the inner layer. The curves well represent the experimental points, indicating that there exists a certain ion-free inner layer in the nitrobenzene solution side of the interface.

The change of γ_{pzc} with $\ln(a^{\pm,NB}_{TBATPB})$ was calculated from

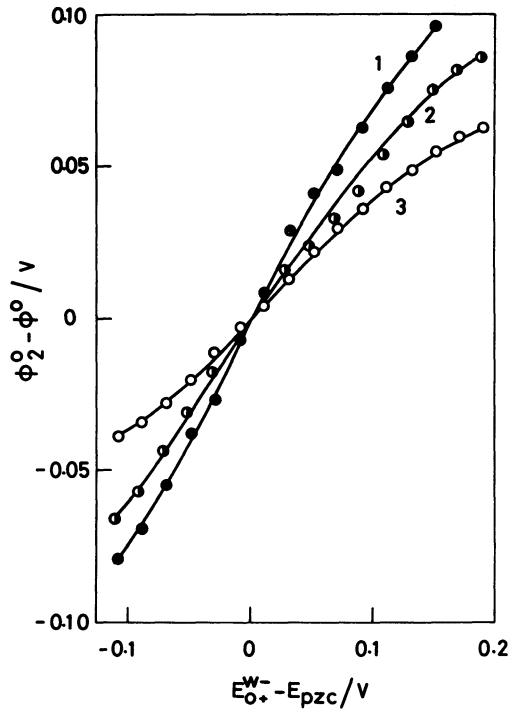

Fig. 10. Potential at outer Helmholtz plane in nitrobenzene solution side of the interface as a function of rational potential difference at (1): 0.02, (2): 0.05, and (3): 0.17 mol dm^{-3} tetrabutylammonium tetraphenylborate.

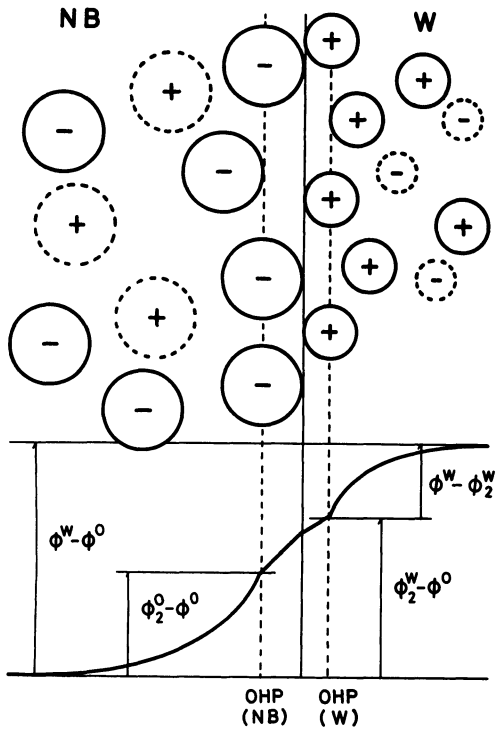

Fig. 11. Schematic representation of the double layer structure and potential profile of the interface between aqueous solution of lithium chloride and nitrobenzene solution of tetrabutylammonium tetraphenylborate.

$$\Gamma_{pzc} = (\Gamma_{pzc})_{c^{NB}_{TBATPB}=0.1} + 2RT\int_{\ln(0.61)}^{\ln(a^{\pm,NB}_{TBATPB})} -(x^{NB}_{TBATPB}/x^{NB}_{NB})^{i}\Gamma_{NB}\, d\ln(a^{\pm,NB}_{TBATPB}). \quad (20)$$

The lower limit of the integration corresponds to $\ln(a^{\pm,NB}_{TBATPB})$ when $c^{NB}_{TBATPB}=0.1$ mol dm^{-3}. The calculated curve well reproduces the experimental data, as shown in Fig. 8.

The Esin-Markov plots at several constant q^W values for the nitrobenzene phase are shown in Fig. 9. The coefficient of the plot when ${}^{i}\Gamma_{TPB}=0$ (or $\partial {}^{i}\Gamma_{TPB}/\partial q^W=0$) and $\partial {}^{i}\Gamma_{NB}/\partial q^W=0$ is given, analogously to the case of the aqueous phase, by

$$\left(\frac{\partial E^{W-}_{O+}}{\partial \ln(a^{\pm,NB}_{TBATPB})}\right)_{q^W,\mu_{j\neq TBATPB}} = -2RT\left(\frac{\partial^{d}\Gamma_{TPB}}{\partial q^W}\right)_{\mu_j} = -\frac{RT}{F}\left(1+\frac{q^W/2}{[(q^W/2)^2+(A^{NB})^2]^{1/2}}\right). \quad (21)$$

Accordingly, the coefficient should reduce to $-2RT/F$, $-RT/F$, and 0 when $q^W \gg 0$, $q^W=0$, and $q^W \ll 0$, respectively. At the pzc, the experimental plot in Fig. 9 has the slope of -24 mV, which is close to $-RT/F=-25.6$ mV. The slope of the plots in Fig. 9 increases with the increase of q^W, which is consistent with the prediction of Eq. 21.

We calculated the potential at the outer Helmholtz plane in the nitrobenzene side (OHP(NB)), ϕ_2^o, referred to the inner potential in the bulk of the nitrobenzene phase, ϕ^o, by using the Gouy-Chapman theory:

$$\phi_2^o - \phi^o = \frac{2RT}{F}\sinh^{-1}[q^W/(2A^{NB})]. \quad (22)$$

The calculated values at three concentrations of TBATPB are plotted in Fig. 10.

Electrical Double Layer at Nitrobenzene–Water Interface. The above discussion shows that in the concentration range and the potential range studied, the adsorption of all the ions at the nitrobenzene–water interface primarily occurs in the diffuse parts of the double layer in both sides of the interface and that there exists an ion-free inner layer between the two diffuse layers. The double layer structure of the interface may then be schematically represented by Fig. 11.

The potential drop across the two inner layers, $\Delta\phi^{W2}_{O2}=\phi_2^W-\phi_2^{NB}$, can be expressed by

$$\Delta\phi^{W2}_{O2} = E^{W-}_{O+} - E_{pzc} - (\phi_2^o-\phi^o) - (\phi^W-\phi_2^W) + \Delta\phi^{W}_{O,pzc}, \quad (23)$$

where $\Delta\phi^{W}_{O,pzc}$ is the inner potential difference between the two phases, *i.e.*, $\Delta\phi^W_O=\phi^W-\phi^O$ at the pzc. The value of $\Delta\phi^{W2}_{O2}-\Delta\phi^{W}_{O,pzc}$ at various concentrations of LiCl and TBATPB are plotted in Fig. 12 as a function of q^W. The experimental points in the positive q^W region are scattered on a single curve with only small deviations. This indicates the virtual invariance of the structure of the inner layer with the change of the concentration of the electrolytes at a given value of q^W and is consistent with the previous conclusion of the absence of ions in the inner layers. The slope of the curve at $q^W=2$ μC cm^{-2} gives the inner layer capacity of 90 μF cm^{-2}, which is in agreement with the value of 83 μF cm^{-2} estimated from the differential capacity measurement of the interface.[19] These values are much higher than the inner layer capacity at the interface between mercury and aqueous solution.[17] Figure 12 also shows that

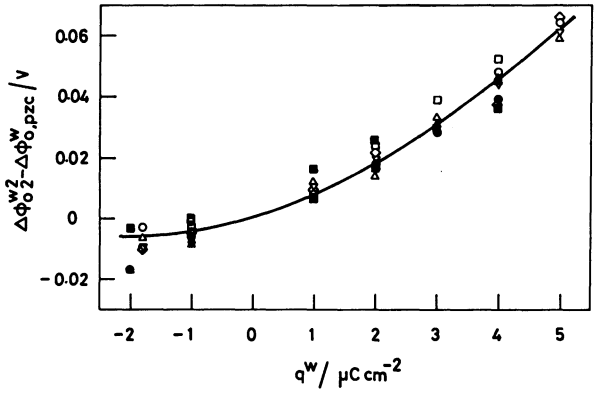

Fig. 12. Change of the inner layer potential difference across the two outer Helmholtz planes $\Delta\phi^{W2}_{02}$ with the change of the surface charge density in aqueous phase at various solution compositions. The concentration of lithium chloride is 0.05 (□), 0.1 (△), 0.2 (◇), 0.5 (▽) and 1.0 (○) mol dm^{-3} when the concentration of tetrabutylammonium tetraphenylborate is 0.1 mol dm^{-3} and the concentration of tetrabutylammonium tetraphenylborate is 0.05 (■), 0.1 (●), and 0.17 (▲) mol dm^{-3} when the concentration of lithium chloride is 0.1 mol dm^{-3}.

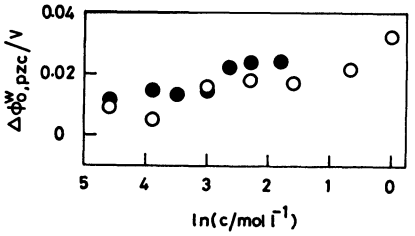

Fig. 13. Potential drop across the two outer Helmholtz planes as a function of the concentrations of tetrabutylammonium tetraphenylborate (●) and of lithium chloride (○).

$\Delta\phi^{W2}_{02}$ increases with the increase of q^W. The slope also becomes larger with increasing q^W, which indicates the decrease of the inner layer capacity with increasing q^W.

The absolute magnitude of $\Delta\phi^{W2}_{02}$ can be evaluated if the value of $\Delta\phi^{W}_{0,pzc}$ is known. In the cell (I) the sum of the potential drops across the phases I and III, and V and VII, $\Delta\phi_I^{III}+\Delta\phi_V^{VII}$, was calculated from the relation: $\Delta\phi_I^{III}+\Delta\phi_V^{VII}=(RT/F)\ln(a^{\pm,W}_{LiCl}/a^{\pm,W}_{TBACl})$. The potential drop across the phase III and IV, $\Delta\phi_{III}^{IV}$, was calculated by the theory of the mixed ion transfer potential[9] to be 247.1 mV when $a=b=0.1$ mol dm^{-3} in the cell (I). In the calculation, simultaneous ion transfer of a primary ion (TBA^+) and its co-ion (Cl^-) in the absence of supporting electrolyte was taken into account and the values of the standard ion transfer potentials of ions from water to nitrobenzene were taken as −0.248 and −0.324 V for TBA^+ and Cl^- ions, respectively.[20] Thus, $\Delta\phi^{W}_{0,pzc}$ was estimated by $\Delta\phi^{W}_{0,pzc}=E_{pzc}-(\Delta\phi_I^{III}+\Delta\phi_{III}^{IV}+\Delta\phi_V^{VII})$. The result is shown in Fig. 13 as a function of the logarithm of the concentrations of TBATPB and LiCl. The $\Delta\phi^{W}_{0,pzc}$ value was always positive and nearly constant at 20 mV when the electrolyte concentration in the two phases was changed. This value is less than one third of the surface potential at the mercury–water interface at the pzc.[21] Such a small surface potential may imply the compensation of the surface potential due to the water dipoles with that of oppositely oriented nitrobenzene dipoles in the inner layer and/or the less oriented structure of the inner layer compared with that at the mercury–water interface.

While this paper was under preparation, Samec *et al.*'s paper[22] on the study of the double structure at the nitrobenzene–water interface appeared. These authors have measured the differential capacity at the interface and analyzed their results with the assumption that the potential at the minimum in the capacity *vs.* potential curve corresponds to the potential of zero charge. However, the capacity minimum occurs at 0.303 V[19] in our system, when $a=b=c=0.1$ mol dm^{-3} in the cell (I), which is 38 mV more positive than the pzc. Also, these authors have estimated $\Delta\phi^{W}_{0,pzc}$ to be 42 mV irrespective of the concentration of LiCl and suggested that the variation of $\Delta\phi^{W2}_{02}$ with q^W is negligible, which is at variance with the present results (see Fig. 12). Gross *et al.*[4] have reported on the basis of the electrocapillary measurements of the non-polarized nitrobenzene–water interface that $\Delta\phi^{W}_{0,pzc}=1$ mV. In their estimation, however, they assumed that the electrocapillary maximum of the non-polarized nitrobenzene–water interface gives the potential of zero charge. This assumption is not generally valid in non-polarized interfaces.[5]

References

1) T. Kakiuchi and M. Senda, *Bull. Chem. Soc. Jpn.*, **56**, 1322 (1983).
2) A. Watanabe, M. Matsumoto, H. Tamai, and R. Gotoh, *Kolloid Z. Z. Polym.*, **220**, 152 (1967).
3) C. Gavach, P. Seta, and B. d'Epenoux, *J. Electroanal. Chem. Interfacial Electrochem.*, **83**, 225 (1977).
4) M. Gros, S. Grom, and C. Gavach, *J. Electroanal. Chem. Interfacial Electrochem.*, **89**, 29 (1978).
5) T. Kakiuchi and M. Senda, to *Bull. Chem. Soc. Jpn.*, in press.
6) T. Kakutani, T. Osakai, and M. Senda, *Bull. Chem. Soc. Jpn.*, **56**, 991(1983).
7) Le Q. Hung, *J. Electroanal. Chem. Interfacial Electrochem.*, **115**, 159 (1980).
8) M. Senda, T. Kakutani, and T. Osakai, *Denki Kagaku*, **49**, 322 (1981).
9) T. Kakiuchi and M. Senda, in preparation.
10) E. A. Guggenheim, "Thermodynamics," 6th ed, North-Holland, Amsterdam (1977), Chap. 5.
11) D. J. Donahue and F. F. Bartell, *J. Phys. Chem.*, **56**, 480 (1952).
12) M. Senda and T. Kakiuchi, paper presented at the 27th Annual Meeting on Polarography, Oct. 1981 (Yokohama) abstract: *Rev. Polarogr. (Kyoto)*, **27**, 49 (1981).
13) C. Davies, "Ion Association," Butterworths, London (1962), p. 39.
14) H. S. Harned and B. B. Owen, "Physical Chemistry of Electrolyte Solutions," 3rd ed, Reinhold, New York (1958), p. 731.
15) J. Kielland, *J. Am. Chem. Soc.*, **59**, 1675 (1937).
16) D. M. Mohilner, "Electroanalytical Chemistry," ed by A. Bard, Marcel Dekker, New York (1966), Vol. 1, p. 321.
17) D. C. Grahame, *Chem. Rev.*, **41**, 441 (1947).

18) R. Parsons, "Advances in Electrochemistry and Electrochemical Engineering," ed by P. Delahay, Interscience, New York (1961), Vol. 1, p. 32.
19) T. Osakai, T. Kakutani, and M. Senda, unpublished result.
20) J. Rais, *Collect. Czech. Chem. Commun.*, **36**, 3253 (1971); J. Rais, P. Selucký, and M. Kyrš, *J. Inorg. Nucl. Chem.*, **38**, 1376 (1976).
21) S. Trasatti, *Croatica Chem. Acta*, **48**, 607 (1976).
22) Z. Samec, V. Mareček, and D. Homolka, *J. Electroanal. Chem. Interfacial Electrochem.*, **126**, 121 (1981).